

Refractories Applications *Transactions*

Volume 2, Number 3

November/December 2006

Editorial Board

Jeffrey D. Smith, Editor, University of Missouri-Rolla, USA
Mary Lee, Assistant to the Editor, University of Missouri-Rolla, USA
William Headrick, University of Missouri-Rolla, USA
Musa Karakus, University of Missouri-Rolla, USA

Technical Referees

Esteban Aglietti, CETMC, Argentina
Richard C. Bradt, The University of Alabama, USA
Carmen Baudín, Instituto de Cerámica y Vidrio, Spain
Elena Brandaleze, Instituto Argentino de Siderurgia
Angel Caballero, Instituto de Cerámica y Vidrio, Madrid, Spain
William G. Fahrenholtz, University of Missouri-Rolla, USA
Geraldo E. Gonçalves, Magnesita S.A., Brazil
Orville Hunter, Consultant, USA
William E. Lee, University of Sheffield, UK
Li Nan, Wuhan University of Sci. & Tech., China
George Oprea, The University of British Columbia, Canada
Victor C. Pandolfelli, Universidade Federal de São Carlos, Brazil
Christopher Parr, Lafarge Aluminates, France
Jacques Poirier, Polytech, Orleans, France
Michel Rigaud, Ecole Polytechnique, Canada
Charles Semler, Semler Materials Services, USA
Mark Stett, Consultant, USA
Raul Topolevsky, Siderar, Argentina

All submissions should be sent to:

Mary Lee, Assistant to the Editor
Refractories Applications Transactions
University of Missouri-Rolla
Materials Science and Engineering Dept.
223 McNutt Hall
1870 Miner Circle Drive
Rolla, MO 65409-0330

Phone: (573) 341-6561
Fax: (573) 341-6934
E-mail: leem@umr.edu

For author guidelines please see those listed on the *Journal of the American Ceramic Society* website: <http://www.ceramics.org/publications/journal/authorinstructions.asp>

File Formats

Text: Microsoft Word.

Graphics: JPEG, TIFF or EPS created from supported applications, PowerPoint, Acrobat PDF (PDF format is acceptable for review purposes only)

Microsoft Word with embedded graphics.

Compression Software: WinZip (PC) or Stuffit (Macintosh)

Resolution of graphics files must be at least 300 dpi for halftones, 600 dpi for lettering, and 1200 dpi for line art.

Influence of Iron Oxides on Corrosion of Refractories Used in Steel Making

Jacques Poirier and Marie Laure Bouchetou

Research Centre for Materials at High Temperature (CRMHT)
Polytech'Orléans, 8 rue L de Vinci 45072 Orléans, France
jacques.poirier@univ-orleans.fr; marie-laure.bouchetou@univ-orleans.fr

1. Introduction

Refractories used in the steel industry must withstand erosion, corrosion, constrained thermal expansion, thermal shock, etc. Degradation results from strong interactions between these chemical, thermal and mechanical phenomena^{1,2}. In general, degradation from corrosion by slags is more extensive than mechanical degradation. Slags are complex mixtures composed of different oxides including lime, silica, alumina and magnesia. However, iron oxides, that are frequently associated with these compounds during steel-making, have a great impact on corrosion.

Phase diagrams are used to study the influence of iron oxides on corrosion of various refractory materials. Four industrial examples will be used to illustrate the role of iron oxides on degradation of bauxite used in torpedo ladles, magnesia used in converters, magnesite-chrome used in RH/OB vacuum degassers and alumina-magnesia refractories used in steel ladles.

2. Effects of iron oxides on refractories

Phase diagrams are invaluable tools that can be used to predict and compare corrosion resistance of different refractories in contact with iron oxides (FeO and Fe₂O₃) aiding in selection of materials for specific steel making applications. Refractories that are most likely to be in contact with iron oxides are high alumina products (fabricated from mullite, bauxite, corundum or tabular alumina) and basic products (fabricated from magnesia, dolomite and magnesite-chrome). The role of iron oxide on the corrosion of these materials is examined from a theoretical point of view.

2.1. Alumina products in contact with iron oxides

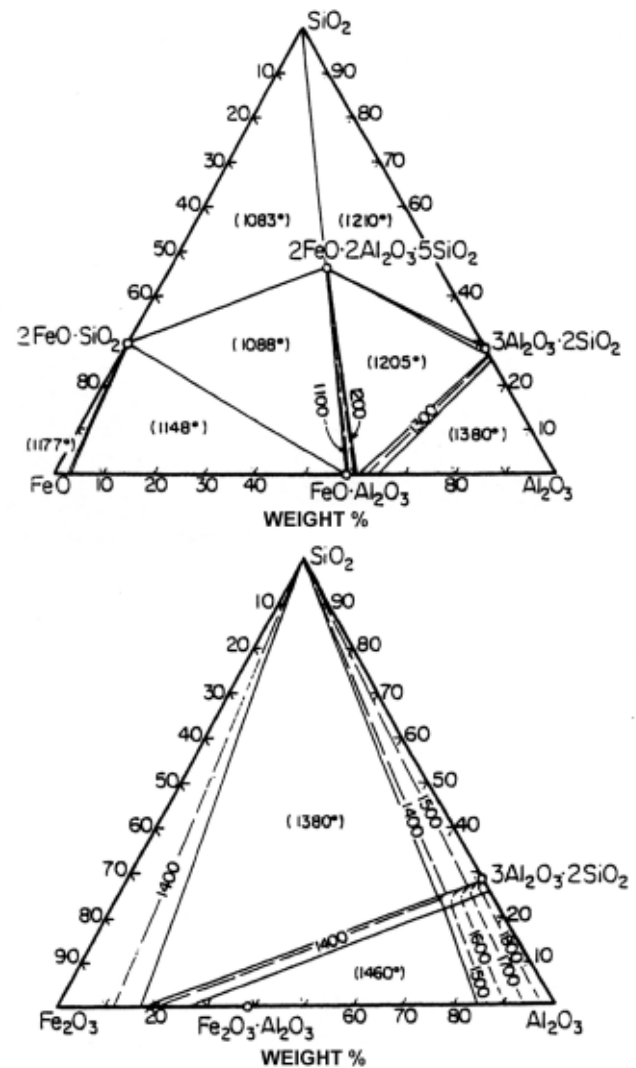
Diagrams for Al₂O₃-SiO₂-FeO and Al₂O₃-SiO₂-Fe₂O₃⁴ reveal the presence of phases with a very low melting points (Figs. 1a and 1b). Corrosion of a fireclay refractory (comprised of mullite and silica) by FeO occurs because a liquid phase forms at the refractory/slag interface even when the temperature is as low as ~1200°C, while in the case of a high alumina refractory (comprised of corundum and mullite) the liquid phase will not appear until a temperature of ~1380°C is reached.

Now, consider the corrosion of an alumina-silicate refractory in contact with an Fe₂O₃ slag. The Fe₂O₃ attack is lesser as the liquid phase forms at a temperature of ~1460°C. Similarly, pure alumina reacts with the iron oxides to form an Al₂O₃-Fe₂O₃ spinel (hercynite) with a high melting point (1740°C). Formation of hercynite has the disadvantage of causing a change in volume that can be harmful to the stability of the refractory.

It can be deduced that (1) alumina and high alumina refractories are sensitive to corrosion by iron oxides because of formation of low melting compounds, (2) iron oxide is more corrosive as the content of alumina in the refractory is lower, and (3) alumina refractories have different degrees of resistance to corrosion by iron oxides depending on the oxygen potential.

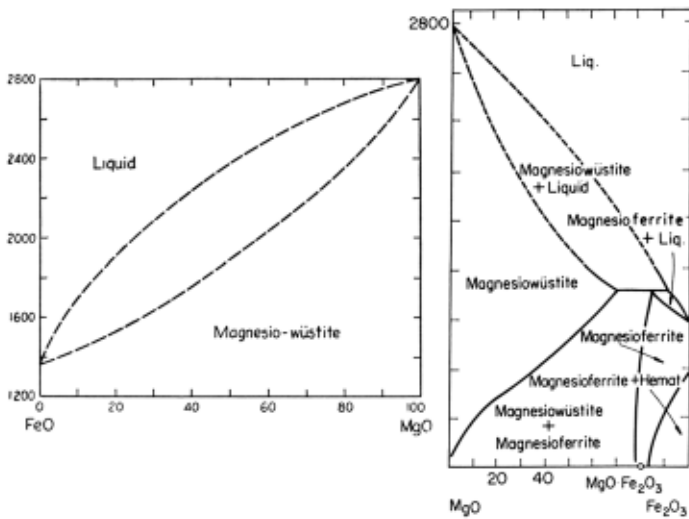
2.2. Basic products in contact with iron oxides

Figs. 2a and 2b show the MgO-FeO and MgO-Fe₂O₃ phase diagrams⁵. Dissolution of magnesia into liquid iron oxides is a complex reaction. Solid reaction products: magnesio-wustite (MgO-FeO) or magnesio-ferrite



Figs. 1a and 1b. Projections of solidus surfaces in the FeO-Al₂O₃-SiO₂ (top) and Fe₂O₃-Al₂O₃-SiO₂ (bottom) systems.

(MgO•Fe₂O₃) occurs at the refractory/liquid iron oxides interface separating magnesia from the slag. At a temperature of 1600°C, MgO can dissolve up to 70 wt% FeO without liquid formation and, even after MgO absorbs ~100 wt% Fe₂O₃, no liquid forms. At 1700°C, MgO can take up ~65% wt% FeO and 70 wt% Fe₂O₃ without developing a liquid phase.

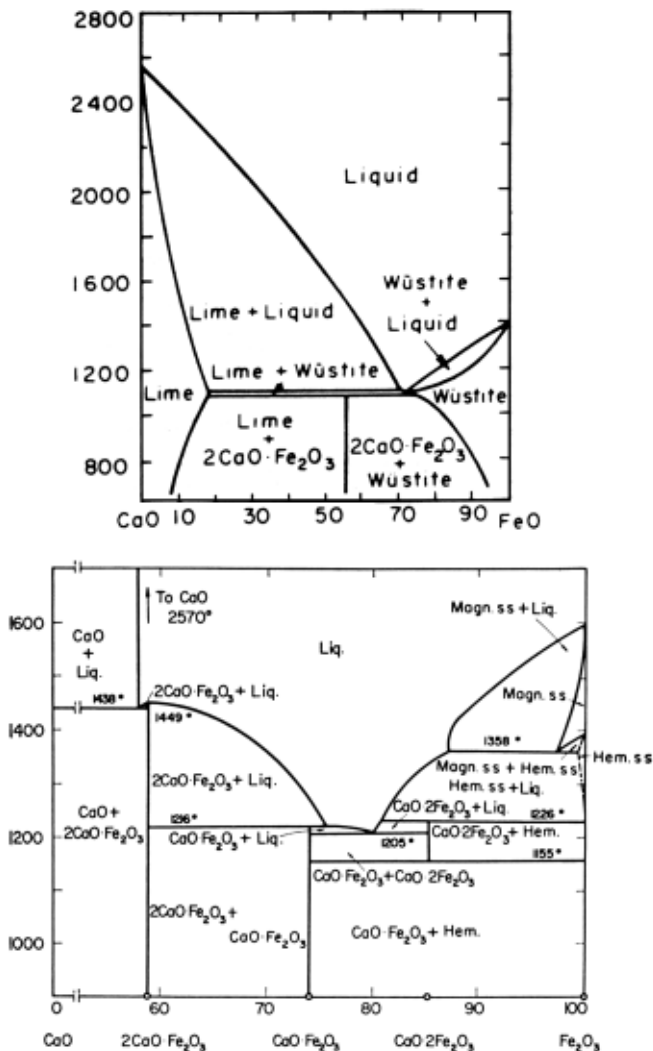


Figs. 2a and 2b. Phase diagrams in the FeO-MgO (left) and MgO-Fe₂O₃ (right) systems.

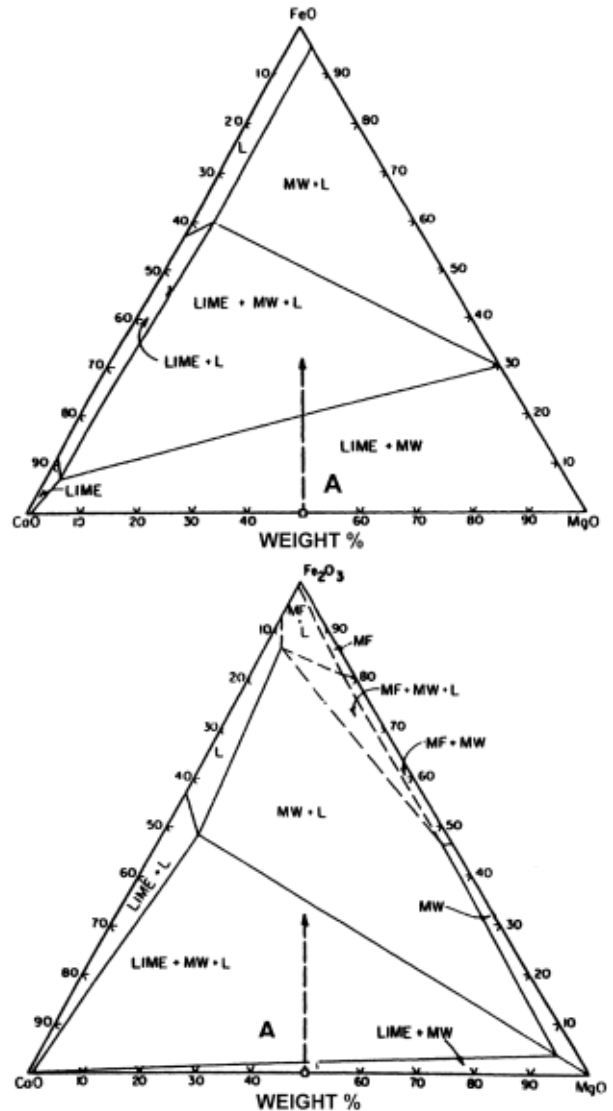
The case of CaO is quite different. As shown in **Figs. 3a and 3b**⁵, iron oxides are corrosive to lime refractories. The presence of even small amount of FeO or Fe₂O₃ fluxes CaO. For example, after CaO dissolves about ~60 wt% Fe₂O₃, the liquidus is ~1450°C. The liquid formation temperature decreases from 2580°C (the melting point of CaO) to 1438°C (solidus) with a small amount of Fe₂O₃. After CaO absorbs only <15 wt% FeO, a liquid will develop at as low as 1160°C. Consequently, MgO refractories are much more resistant to iron oxides than CaO refractories.

Considering the corrosion resistance of dolomite (MgO-CaO) refractories in contact with iron oxides, **Figs. 4a and 4b** show the MgO-CaO-FeO and MgO-CaO-Fe₂O₃ phase diagrams⁴ at a temperature of 1500°C. These diagrams reveal a great difference in the extent of the zone of the liquid phase according to the degree of iron oxidation.

Dolomite (composition A in **Figs. 4 and 4b**) can dissolve approximately 22 wt% ferrous oxide (FeO) without a liquid phase developing at 1550°C. Only 3 wt% ferric oxide (Fe₂O₃) develops a liquid phase at the same temperature. To improve corrosion resistance, carbon is often added in dolomite refracto-



Figs. 3a and 3b. Phase diagrams in the CaO-FeO (top) and CaO-Fe₂O₃ (bottom) systems.



Figs. 4a and 4b. 1500°C isothermal sections in the MgO-CaO-FeO (top) and MgO-CaO-Fe₂O₃ (bottom) systems.

ries. Indeed, carbon, mainly present as graphite or pyrolysed carbon from resin or pitch, in MgO-CaO-C refractories, has a beneficial effect of corrosion by iron oxide. The carbon reduces some of the iron oxides and limits the formation of low melting phases. In addition, the non wettability of carbon limits the liquid slag penetration.

For the magnesia-chrome products, MgO-FeO-Fe₂O₃ and MgO-FeO-Fe₂O₃-Cr₂O₃ diagrams⁶ (Figs. 5a and 5b) show the influence of an addition of chromium oxide on the corrosion of magnesia refractories in the presence of iron oxide. With higher Cr₂O₃ content, the corrosion is lower. We notice an extension of the spinel Mg(Cr,Fe)₂O₃ region and a reduction of the solid solution MgO-FeO area. With high oxidizing conditions, the temperatures of liquidus strongly rise for high values of iron oxide. Magnesite-chrome products are less sensitive than magnesia products to the influence of the oxygen partial pressure.

Now consider both the influence of a basic slag (CaO/SiO₂ >2) and of iron oxide on the corrosion of magnesia and magnesia-chrome refractories. The Ca-Fe-Mg-Si-O diagram⁷ (Fig. 6) shows that magnesia does not have an exceptional behavior. A liquid phase will be developed at as low as 1380°C. The case of the magnesia chrome refractory is quite different. As shown in Figs. 7a and 7b, the addition of Cr₂O₃ to magnesia refractories (formation of MgO•Cr₂O₃ magnesio-chromite spinel) has a positive effect on corrosion

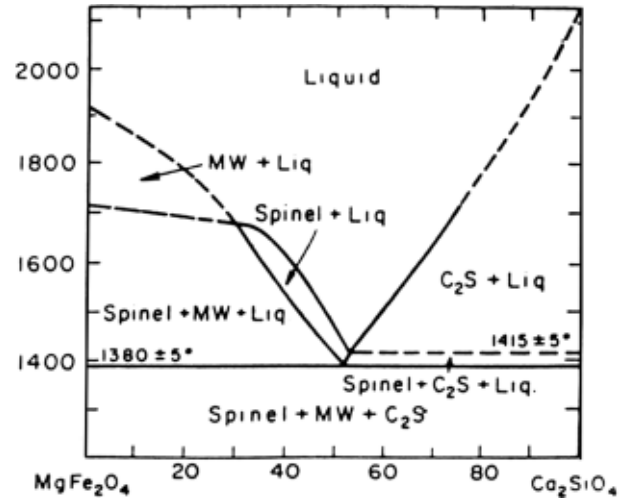
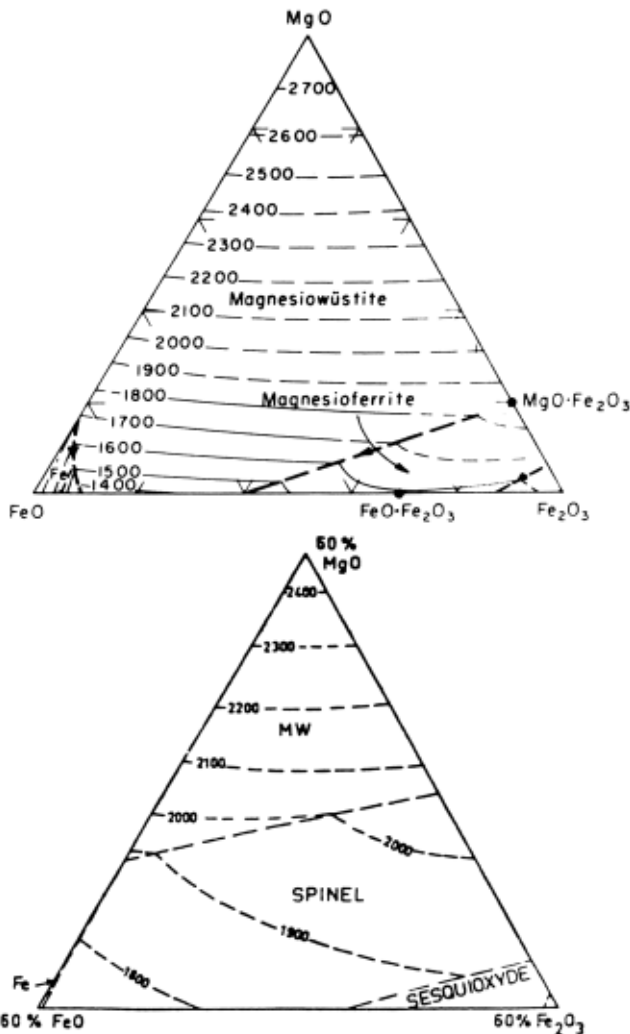
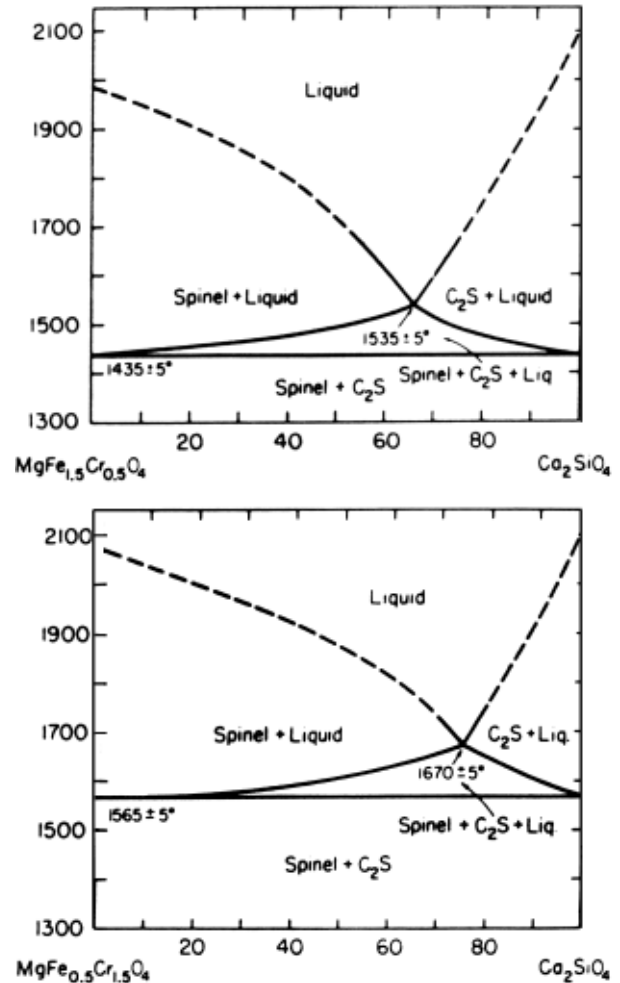


Fig. 6. Pseudobinary diagram in the Ca₂SiO₄-MgFe₂O₄ system, where C₂S is Ca₂SiO₄ and MW is magnesio-wüstite.



Figs. 5a and 5b. Liquidus surfaces in the MgO-FeO-Fe₂O₃ (top) and MgO-FeO-Fe₂O₃-40 wt% Cr₂O₃ (bottom) systems.



Figs. 7a and 7b. Pseudobinary diagrams in the MgF_xCr_{1-x}O₄-Ca₂SiO₄ system.

resistance⁷. The liquid formation temperature increases up to 1535°C (temperature of solidus of the $\text{MgFe}_{0.5}\text{Cr}_{1.5}\text{O}_4\text{-Ca}_2\text{SiO}_4$ diagram). However, the chromite raw materials used in magnesia-chrome refractories contain alumina as secondary phase, which lowers the fusion range and has a negative influence on corrosion⁸. The temperature of the solidus decreases down to 1455°C (Fig. 8).

3. Corrosion of industrial refractories by iron oxides

Industrial examples of corrosion by iron oxides are analyzed using the relevant phase diagrams discussed previously.

3.1. High alumina linings in torpedo ladles⁹

During draining of pig iron, slag in contact with the refractory surface infiltrates the porosity, up to the isotherm of solidification. The result is a modification of the characteristics of the refractories, particularly the coefficient of expansion and the thermomechanical properties. During thermal cycles from repeated fillings and drainings, there are high mechanical stresses at the interface between the unaffected area and the impregnated part of the brick, which generate cracks and a consequent irregular wear of the lining, as shown on Fig. 9. These impregnation-spalling phenomena appear in all the immersed parts of the torpedo ladles but are more visible in those areas where thermal

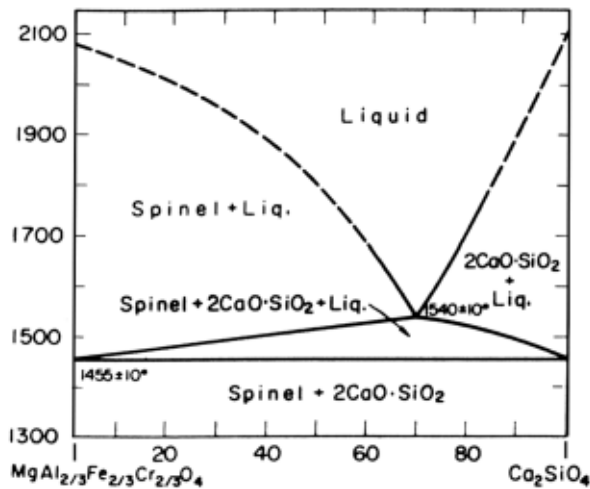


Fig. 8. Section $\text{MgAl}_{0.67}\text{Fe}_{0.67}\text{Cr}_{0.67}\text{O}_4\text{-Ca}_2\text{SiO}_4$ of the quaternary diagram $\text{MgAl}_2\text{O}_4\text{-MgFe}_2\text{O}_3\text{-MgCr}_2\text{O}_4\text{-Ca}_2\text{SiO}_4$.

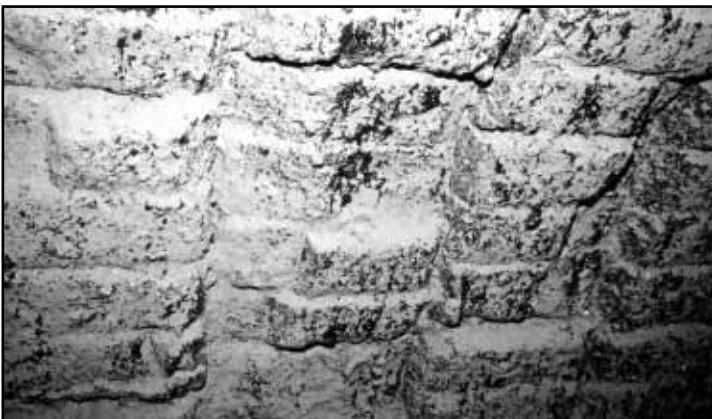


Fig. 9. Structural spalling of a torpedo ladle lining.

shocks are higher (central region) or in heavily insulated areas (bottom). Reduced slag penetration yields greater resistance to impregnation-spalling.

In addition to the damage by impregnation-scaling, there is damage of the refractory material by the slag. Not only is it the main mechanism in the slag level area, but it is also present in all the zones touched by the slag during the torpedo ladle draining. After the desulphurization process, the torpedo ladle slags contain variable percentages of metallic iron: 10 to 20 wt% of the slag composition. The iron comes from projections of metal caused by the violent agitation caused by the desulphurization process. During the repetitive thermal cycles: heating-cooling, the iron in the slag can be oxidized with obvious consequences on the corrosion of the high alumina content bricks.

At the lower end of the cones, wear of the bricks joints can be noted (Fig. 10). This wear profile can be explained by (1) modification of the surface of bricks from infiltration of slag that causes shrinkage and risk of penetration at the joints, (2) corrosion by reduction of silica-containing compounds in the refractory by desulfurization agents, and (3) selective erosion of the bricks joints by turbulence of the pig iron.

The inspection of the linings during and at the end of the campaigns as well as the study of the used bricks makes it possible to define the effects of iron oxides in order to analyze the various stresses encountered in torpedo ladles. Table 1 compares the chemical analysis and the physical properties of a clay bonded bauxite refractory before and after use in the impact zone. The brick properties are changed by the presence of a phase with a high iron oxide content of the composition 56 wt% SiO_2 , 20 wt% MnO , 15 wt% FeO , 4 wt% CaO , and 5 wt% accessory oxides. This phase has a double function (1) it has a low melting onest temperature so it impregnates the brick deeply and (2) it promotes the densification and shrinkage of the brick.

Both micrographic examination (Fig. 11) and microanalyses carried out with an electron microscope show the various phenomena involved:

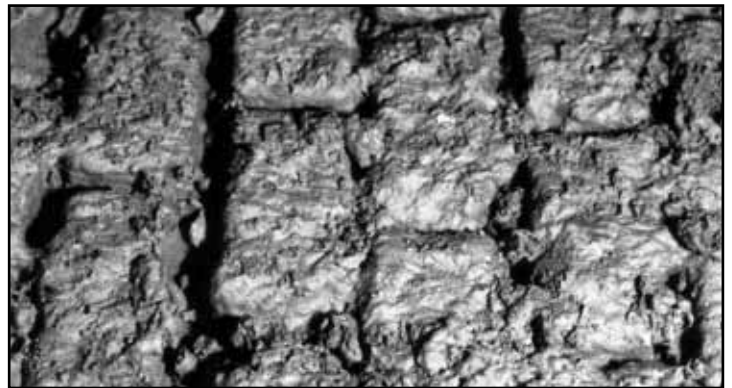


Fig. 10. Corrosion of the joints at the lower part of the cones.

Table 1. Chemistry and physical properties of high alumina refractory used in torpedo ladles.

	Before use	After use
Fe_2O_3	1.6	5.28
SiO_2	13.5	20.34
Al_2O_3	81.8	68.42
CaO	0.1	0.82
MgO	0.2	0.21
MnO	0.1	2.95
TiO_2	2.96	2.4
Density (kg/m^3)	2.81	3.68
Porosity (vol%)	19.2	3.57

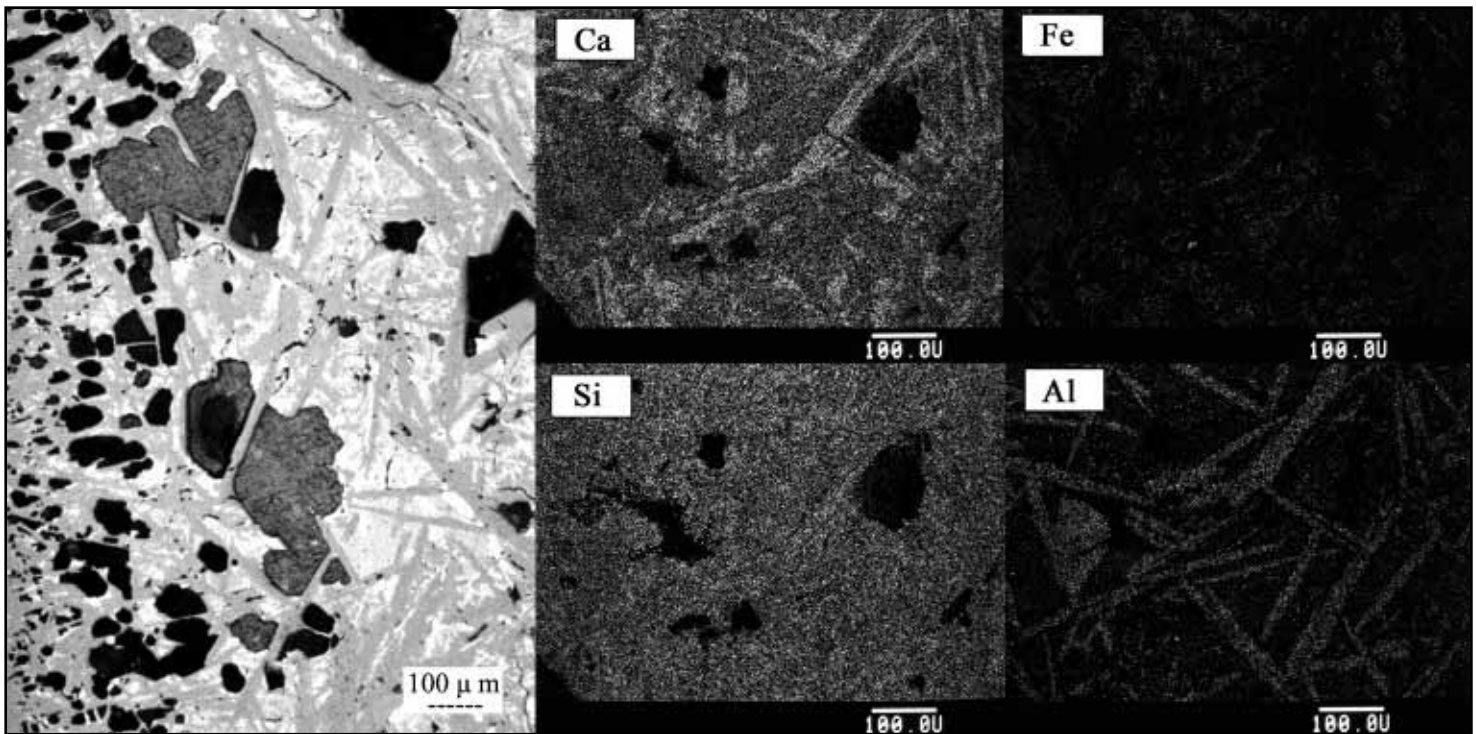


Fig. 11. SEM micrograph (left) of the hot face of a corroded bauxite brick and the associated EDS compositional maps for Ca, Fe, Si and Al.

- a transformation of the bauxite grains in contact with the slag, with the recrystallization of long needles (200 to 300 μm) of anorthite ($\text{CaO} \cdot \text{Al}_2\text{O}_3 \cdot 2\text{SiO}_2$) or hexa aluminate of lime ($\text{CaO} \cdot 6\text{Al}_2\text{O}_3$).
- the presence of iron oxide can also be noted, partly diffused in a vitreous phase $\text{CaO-SiO}_2\text{-FeO}$ (with a fluidizing action) and in the form of free nodules or nodules associated with lime or alumina. In this context, it is easier to understand the increasing use of carbon-based refractories: either post-impregnated for fired refractories or carbon bonded with graphite incorporation for alumina-carbon-silicon carbide refractories, which acts favorably on the wettability of the refractory by the slag and also has a positive action on the reduction of iron oxides in contact with the refractory.

3.2. Magnesite carbon converter linings¹⁰

Corrosion mechanisms of MgO-C refractories used in BOF linings include (1) Formation of a decarburized layer through reaction of carbon species with the oxygen atmosphere or with FeO in the slag, (2) infiltration of slag into decarburized layer and subsequent erosion of the magnesite grains, and (3) dissolution and reaction of matrix bonding magnesite crystals.

Fig. 12 shows the microstructure of a MgO-C brick after use in the slag line of a converter. This microstructure indicates (1) dissolution of magnesite by iron oxides and formation of magnesio-wustite solid solution, which causes a harmful change in volume, (2) infiltration of slag that reacts with the intercrystalline silicate phases to yield compounds with low melting points, and (3) destruction of silicate bonds and/or direct bonds leading to dissolution of crystallites into the slag.

3.3. Magnesite-chrome lining in RH/OB vacuum degasser¹¹

The vacuum degasser units are used to produce extra low carbon deep drawing steels for automotive customers (I-F Steels). These units are required to vacuum decarburize and homogenize the heat, as well as be a ladle metallurgy station with final additions of alloys being made to satisfy stringent metallurgical requirements. These activities put great strain upon refractory

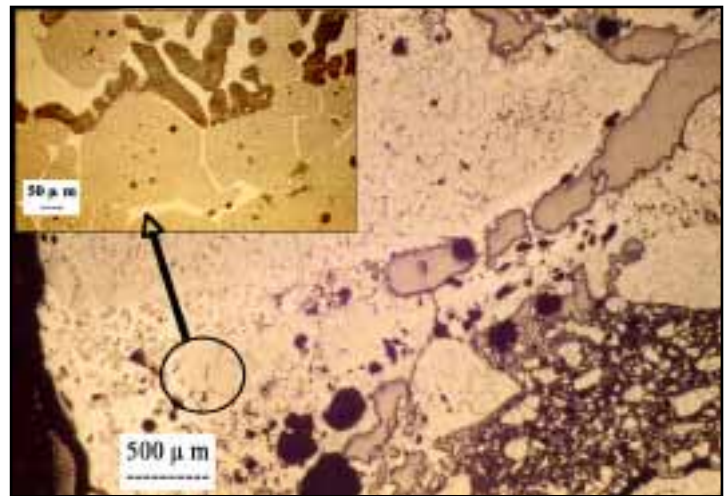


Fig. 12. Microstructure of a MgO-C brick after use in the slag line of a converter.

materials. Fig. 13 shows a general view and plan of the brickwork of a vacuum degasser.

Deep vacuum treatment gives rise to steel projections on the inside of the vessel, which results in the formation of skulls at the level of the intermediate ring. For good operation of the RH/OB degasser, these must be regularly eliminated. The technique used is that of an oxygen lance which oxidizes and melts the skull. The iron oxides formed during the top-oxygen blowing, are brought to a very high temperature, are very liquid, and hence impregnate the refractory products and cause severe corrosion. Such corrosion in connection with cyclic temperature variations causes the structural spalling of the affected layer (Fig. 14).

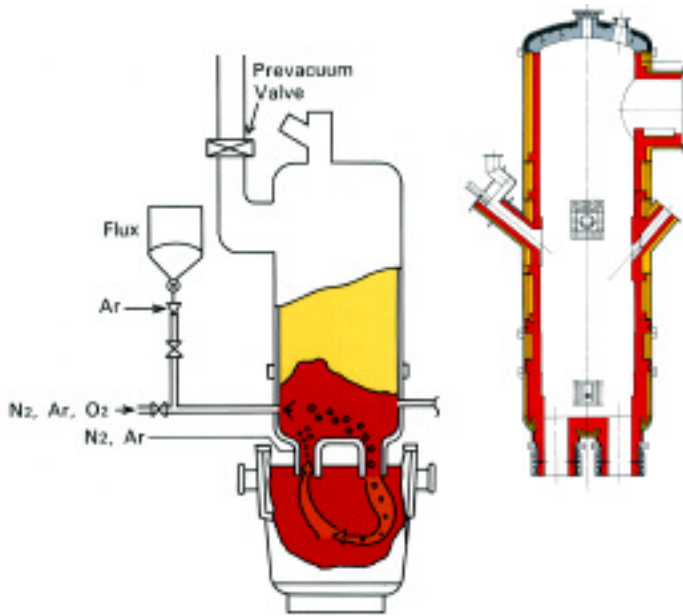


Fig. 13. General view and plan of the brickwork of a vacuum degasser (RH/OB).



Fig. 14. Used magnisite-chrome brick with structural spalling damage.

Vacuum treatment also causes a risk of air leakage at imperfect joints. This air leakage causes highly localized and deep wear which can be dangerous since it is unpredictable as shown in Fig. 15. Air leakage shows up in the vessel mainly at connections between the different parts of the structure, but may also be channeled behind the lining and emerge through a slightly opened joint between two bricks at any spot on the lining. The corrosion is due to exothermic reactions at the contact between the melted refractory and the metal as well as the strong turbulence which arises at the point of air leakage into the vessel. Effects of iron oxides are of two types, (1) those formed during desulfuring lead to regular corrosion/impregnation, and (2) those formed by oxygen aspiration lead to an intense corrosion process.

The wear process has been examined through observation of the refractory linings of the RH/OB installations while in use as well as by examination of used samples. The observations have clearly shown different factors of corrosion, namely the presence of iron oxides and attack of slag, impregnation-spalling, and (3) the influence of vacuum and atmosphere.

Observing the structure of used samples (Fig. 16) reveals a shiny corroded area with a thickness of 1-2 mm. The periclase grains were saturated with



Fig. 15. Corrosion of a RH/OB lining due to air leakage.

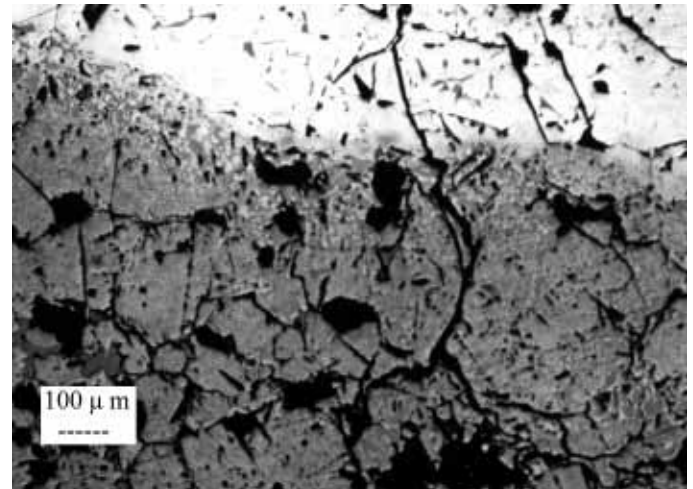


Fig. 16. Microstructure of the hot face of a magnesia-chrome refractory after use.

iron oxide, associated with a swelling effect with dislocations and the formation of compounds with a melting point lower than the treatment temperature. This leads to superficial wear of the brick by structural spalling.

By comparing x-ray diffraction spectra obtained on samples taken respectively from near the hot face, behind the used bricks, and from new bricks, the following evolution is also shown

- an evolution of the spinel composition between a solid solution of the $(Mg Fe)(Cr Al)_2 O_4$ type for the new brick and a solution of the type $Mg(Al Fe)_2 O_4$ for an area located near the corrosion front,
- that this evolution results in the disappearance of the chrome.

The wear mechanism of the magnesite-chrome bricks in the RH/OB is strongly linked to the presence of oxygen and may be broken down as follows:

- volatilization of the chromium oxide is higher when the oxygen partial pressure is high. This is due to the existence of gaseous chromium oxides richer in oxygen than Cr_2O_3 (CrO_2 and CrO_3 vapors).
- on the surface, infiltration of iron oxide and calcium silicates with formation of magnesio-ferrite and magnesio-ferrite with a dissolution of magnesia.

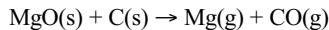
Examination of the equilibrium diagrams provides an explanation of the behavior of magnesite-chrome products and of the role of iron oxide and, possibly, of oxygen. Without Cr_2O_3 , it may be noted that it is possible to have a liquid phase in the $\text{MgO-Fe}_2\text{O}_3\text{-FeO}$ system from 1400°C to 1600°C (Fig. 5a). With Cr_2O_3 , the disappearance of the liquid phase may be noted. This explains the favorable role of this addition (Fig. 5b). If a lime slag is superposed on iron oxides, diagrams in Figs. 7a and 7b show that the temperature of appearance of the first liquid phase decreases when the Fe_2O_3 content increases, to the detriment of the Cr_2O_3 . In the presence of infiltrated slag and iron oxides, all of these phenomena contribute to an accelerated wear of the refractories through the formation of melting phases in the fragile area by volatilization of chrome oxide.

With respect to the observations made, it appears important to master the technique of deskulung in order to reduce the effect of iron oxides and to select magnesite-chrome products to reduce the tendency to impregnation, and thus spalling.

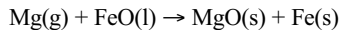
3.4. Magnesia-carbon and alumina-spinel in steel ladles¹²

Certain steels, such as ultra-low carbon steels require a high oxygen content during decarburization (CO degassing) and the slag line of the steel ladle has long lasting contact with iron oxide rich slag. The presence, in a limited amount, of these iron oxides in the slag can have a beneficial effect on the corrosion of magnesia carbon bricks used in the ladles. Indeed, in contact with FeO , a protective dense MgO layer^{13,14} can be formed on the hot face of the MgO-C refractories as shown in Fig. 17.

Inside the magnesia carbon brick, the following reaction occurs:



At high temperature, magnesia is reduced by the carbon to form Mg vapor that is transported to the hot face where it is oxidized to a secondary MgO dense layer by reduction of iron oxides and precipitation of iron.



Careful control of service conditions such as the level of iron oxidation (FeO , Fe_2O_3) and the composition of the slag is required to trigger formation of a secondary MgO dense layer.

Spinel forming magnesia alumina castables have been developed and are used successfully in the impact pad of steel ladles. Based on the analysis of refractories used in the ladles, the effect of spinels to limit the corrosion by iron oxides is described. Fig. 18 shows a microstructure of the hot face of an alumina magnesia castable after use. Alumina reacts with the lime of the slag to form a new phase: $\text{CaO-6Al}_2\text{O}_3$ which has a very high melting point. The

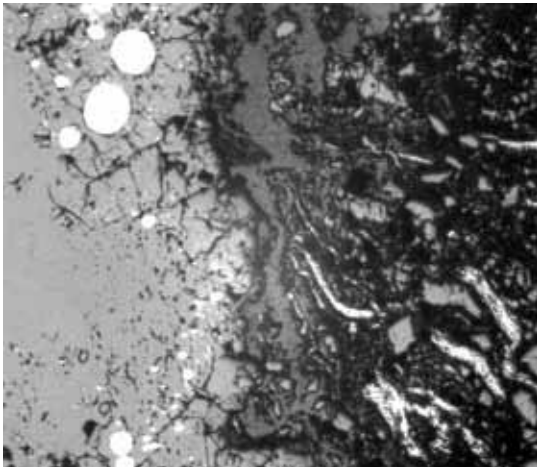


Fig. 17. Microstructure of a MgO dense layer at the hot face of a magnesia-carbon refractory.

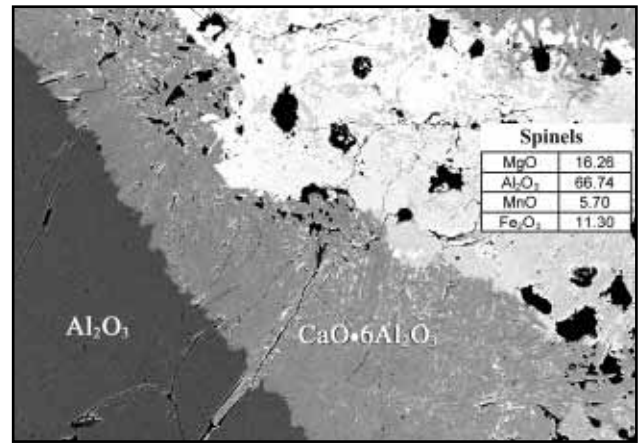


Fig. 18. Microstructure of the hot face of an alumina magnesia castable.

spinel reacts with iron oxide and manganese oxide compounds in the slag to form a solid solution of spinel: $(\text{Mg,Fe,Mn})\text{O}(\text{Al}_2\text{Fe}_2)\text{O}_3$. The composition of the slag changes and its viscosity becomes high. As the result, the penetration is limited because of a rise in both the high melting point and the viscosity.

4. Conclusion

The influence of iron oxides on the corrosion resistance of various refractory materials has been studied using phase diagrams. These diagrams provide useful data to interpret and predict the mechanisms of corrosion in different industrial applications. Microstructure studies of refractories after use show a good agreement with these phase diagrams.

References

- ¹J. H. Chesters, "Refractories, Production and Properties," The Metals Society, London, 1983.
- ²C. A. Schacht, "Refractory Linings: Thermomechanical Design and Applications-Mechanical Engineering," Dekker M. INC., New York, USA, 1995.
- ³S. Zhang, W. E. Lee, "Use of Phase Diagrams in Studies of Refractories Corrosion," *Int. Mater. Rev.*, **45** [2] 41-58 (2000).
- ⁴A. Muan, E. F. Osborn, "Phase Equilibrium Among Oxides in Steelmaking," Reading, MA, Addison-Wesley, 1965.
- ⁵E. M. Levin, C. R. Robbins, H. F. McMurdie, M. K. Reser, "Phase Diagrams for Ceramists," Columbus, OH, American Ceramic Society, 1964.
- ⁶B. Phillips and A. Muan, "Phase Equilibrium in the System $\text{MgO-FeO-Fe}_2\text{O}_3$ in Temperature range $1400\text{-}1800^\circ\text{C}$," *J. Am. Ceram. Soc.*, **45** 588-91 (1962).
- ⁷R. M. El-Shahat, J. White, "Systems $\text{MgAl}_2\text{O}_4\text{-MgCr}_2\text{O}_4\text{-Ca}_2\text{SiO}_4$ and $\text{MgFe}_2\text{O}_4\text{-MgCr}_2\text{O}_4\text{-Ca}_2\text{SiO}_4$," *Trans. Brit. Ceram. Soc.*, **63** [6] 313-330 (1964).
- ⁸R. M. El-Shahat, J. White, "Phase-Equilibrium Relationships in Spinel-silicate Systems II. The Pseudo-Systems $\text{MgAl}_2\text{O}_4\text{-MgCr}_2\text{O}_4\text{-CaMgSiO}_4$, $\text{MgFe}_2\text{O}_4\text{-MgCr}_2\text{O}_4\text{-CaMgSiO}_4$, $\text{MgAl}_2\text{O}_4\text{-MgFe}_2\text{O}_4\text{-CaMgSiO}_4$, and $\text{MgAl}_2\text{O}_4\text{-MgFe}_2\text{O}_4\text{-MgCr}_2\text{O}_4\text{-CaMgSiO}_4$," *Trans. Brit. Ceram. Soc.*, **65** [6] 309-336 (1966).
- ⁹J. Poirier, M. Frère, J.M. Chatillon, G. Leduc, "The Development of 450-Ton Torpedo Ladle Linings at Sollac Dunkerque, n° 2 Steel Works," pp. 46-53 in Proceedings of 31st International Colloquium on Refractories, German Refractory Assoc. Edit., Aachen, (1988).
- ¹⁰J. Poirier, F. Etienne, F. Masse, "Role of Raw Materials and Properties of Magnesia Carbon Bricks in the Wear Mechanism of LD Converter Refractory Lining," pp. 336-347. *UNITECR 89 Proceedings of Unified International Technical Conference on Refractories*, American Ceramic Society Edit., Anaheim, 1989.
- ¹¹D. Brachet, F. Masse, J. Poirier, G. Provost, "Refractories behavior in the Sollac Dunkirk RH/OB Steel Degasser," *J. Can. Ceram. Soc.*, **58** [4] 61-66 (1989).
- ¹²J. Poirier, M. Rigaud, "The Stability of Metals, Carbides and Oxides in Carbon Magnesia refractories," *J. Can. Ceram. Soc.*, **62** [1] 70-76 (1993).
- ¹³W. E. Lee, S. Zhang, "Melt Corrosion of Oxide and Oxide-Carbon Refractories," *Int. Mater. Rev.*, **44** [3] 77-104 (1999).
- ¹⁴R. H. Herron, C. R. Beechan, R. C. Padfield, "Slag Attack On Carbon-Bearing Basic Refractories," *Am. Ceram. Soc. Bull.*, **46** [12] 1163-1168 (1967).